

Measuring Fractional Charge in Carbon Nanotubes

Cristina Bena,¹ Smitha Vishveshwara,¹ Leon Balents,¹ and Matthew P. A. Fisher²

Received August 14, 2000

The Luttinger model of the one-dimensional Fermi gas is the cornerstone of modern understanding of interacting electrons in one dimension. In fact, the enormous class of systems whose universal behavior is adiabatically connected to it are now deemed Luttinger liquids. Recently, it has been shown that metallic single-walled carbon nanotubes are almost perfectly described by the Luttinger Hamiltonian. Indeed, strongly non-Fermi liquid behavior has been observed in a variety of DC transport experiments, in very good agreement with theoretical predictions. Here, we describe how *fractional quasiparticle charge*, a fundamental property of Luttinger liquids, can be observed in impurity-induced shot noise.

KEY WORDS: Carbon nanotubes; Luttinger liquids; charge fractionalization; shot noise; non-equilibrium measurements.

1. INTRODUCTION

The study of interacting electrons in one dimension has opened a panoply of surprises which often seem counter-intuitive from the perspective of higher dimensions. The generic behavior of one-dimensional metals is that of the *Luttinger liquid*.^(1, 2) In a Luttinger liquid, interactions conspire to host bizarre phenomena such as the separation of spin and charge, as well as anomalous power-law dependences in the resistivity and density of states. Perhaps the most fundamental difference between the Luttinger liquid and higher-dimensional metals lies in the nature of its quasiparticles. The Luttinger quasiparticles are “fractionalized,” and indeed the elementary

¹ Department of Physics, University of California, Santa Barbara, California 93106.

² Institute for Theoretical Physics, University of California, Santa Barbara, California 93106-4030.

charged quasiparticle carries not the quantum of charge “ e ” of the electron, but instead, a fraction “ ge .”

While the exploration of Luttinger liquid physics began more than half a century ago,^(1,2) it has only found its way into the experimental realm in the past decade. The quantum Hall system with its chiral edge states has championed displaying Luttinger liquid features.⁽³⁾ In particular, it has provided the definitive confirmation of the existence of fractional charge through shot noise measurements.⁽⁴⁾ However, the challenge of finding a truly one-dimensional (1D) system of interacting electrons has persisted. A variety of transport experiments^(5–9) now convincingly demonstrate that single-walled carbon nanotubes (SWNTs) behave as Luttinger liquids, as predicted theoretically.^(10,11)

Here, we show that even the simple set-up of a clean armchair nanotube with a single weak impurity is capable of flaunting a hallmark of Luttinger liquids, namely charge fractionalization. To understand the physical meaning of charge fractionalization, consider a simple thought experiment in which electrons are sequentially transferred from a metallic electrode onto the end of a nanotube through a large contact barrier. With a sufficiently high barrier, the rate of charge addition can be made very low, so that each incident electron can be considered individually. Immediately after the addition event, the added charge e travels as a solitonic pulse away from end of the nanotube (incidentally, the added spin $\hbar/2$ travels as separate *slower* soliton behind the charge). This charge e soliton may be regarded as the remnant of the electron in the nanotube. Upon reaching an impurity, however, the true nature of the charge excitations of the Luttinger liquid becomes evident. In a non-interacting system, an incident particle either transmits (with probability T) or reflects (with probability $R = 1 - T$). In the nanotube, the charge e soliton can still transmit (with probability T), but the alternative possibility (which is the leading-order scattering process occurring with probability $\approx 1 - T$ for a weak impurity) is to “splinter” into *two* solitons: a backscattered piece of charge ge and a transmitted piece of charge $(1 - g)e$. The dimensionless “Luttinger parameter” g ($g < 1$ for repulsively interacting Fermi systems) depends on the nature of the interactions in the system. In carbon nanotubes, theoretical estimates give $g \approx 0.2$ ¹⁰, in good agreement with transport measurements.^(5–9)

Unfortunately, the difficulty of the necessary time-resolved measurements makes the above thought experiment impractical. Nevertheless, as shown in the next section, the mathematics of Luttinger liquid theory leaves no room to doubt that such strange scattering events indeed occur. In this paper, we determine the consequences of these processes for *shot noise*. Strikingly, we find that at low enough temperatures, fluctuations in the net current incident on the weak barrier have the shot noise form

appropriate for Poisson distributed scattering events of particles of charge ge . Measurements of such shot noise are more tractable, and can provide definitive proof of charge fractionalization.

As elucidated in what follows, to experimentally observe the described shot noise, we propose a four terminal set-up capable of measuring correlations in current C_I , and the voltage drop V across an impurity placed along the nanotube. In the limit of zero temperature, we derive the relationship $C_I = 4g^2(e^3/h)V$; C_I is related to the backscattered current I_B via $C_I = geI_B$, while I_B is given by $I_B = 4g(e^2/h)V$. Thus one can extract the charge fraction g . The SWNT, with its estimated value $g \approx 0.2$ far from unity, makes for an exquisite playground to test the predicted Luttinger liquid physics, specifically, the fractionalization of charge.

2. FORMALISM

To extract the non-equilibrium physics of the set-up described above, we formulate an effective time-dependent theory for the bulk of the nanotube and for the impurity site. The effective theory of the clean single-walled nanotube in consideration may be described by the low energy physics of the (N, N) armchair tube. In the absence of interactions, this involves two gapless one-dimensional metallic bands modeled by free fermions with linear dispersion:⁽¹⁰⁾

$$H_0 = \sum_{i, \alpha} \int dx v_F [\psi_{Ri\alpha}^\dagger i \partial_x \psi_{Ri\alpha} - \psi_{Li\alpha}^\dagger i \partial_x \psi_{Li\alpha}] \quad (1)$$

where v_F is the Fermi velocity, R and L label the right and left movers respectively, $i = 1, 2$ label the bands, and $\alpha = \uparrow, \downarrow$ the electronic spin. In this section, we set $\hbar = e = 1$.

The bosonized version of the fermionic operators has the form $\psi_{R/Li\alpha} \sim e^{i(\phi_{i\alpha} \pm \theta_{i\alpha})}$. A more convenient basis, which we employ extensively, involves a spin and channel decomposition for θ : $\theta_{i, \rho/\sigma} = (\theta_{i\uparrow} \pm \theta_{i\downarrow})/\sqrt{2}$ and $\theta_{\mu\pm} = (\theta_{1\mu} \pm \theta_{2\mu})/\sqrt{2}$ with $\mu = \rho, \sigma$, and a similar one for ϕ . The new fields obey the canonical commutation rules $[\phi_a(x), \theta_b(y)] = -i\pi\delta_{ab}\Theta(x-y)$, with $a, b = (\rho+, \rho-, \sigma+, \sigma-)$. As discussed in ref. 10, interactions effectively involve just the charge density, $\rho = (2/\pi)\partial_x\theta_{\rho+}$. The entire Hamiltonian density ($H = \int dx \mathcal{H}$), with interactions taken into account, then has the bosonized form:

$$\mathcal{H} = \sum_a \frac{v_a}{2\pi} [g_a^{-1}(\partial_x\theta_a)^2 + g_a(\partial_x\phi_a)^2] \quad (2)$$

with $g_{\rho+} \equiv g = v_F/v_{\rho+} < 1$, and $g_a = 1$, $v_a = v_F$ for $a \neq \rho+$. In terms of the right- and left-moving chiral modes $\Phi_a^{R/L} = g_a \phi_a \pm \theta_a$, one has associated densities $n_a^{R/L} = \pm (1/\pi) \partial_x \Phi_a^{R/L}$.⁽¹²⁾ The above Hamiltonian density now takes the diagonal form:

$$\mathcal{H} = \sum_a \left\{ \frac{\pi v_a}{4g_a} [(n_a^R)^2 + (n_a^L)^2] \right\} \quad (3)$$

with corresponding equations of motion

$$(\partial_t \pm v_a \partial_x) n_a^{R/L} = 0 \quad (4)$$

Thus, the density propagates as a one-dimensional acoustic plasmon with renormalized velocity $v_{\rho+}$. The parameter g depends on the ratio of the Coulomb energy between particles and the Fermi energy, and in a SWNT has the approximate value of 0.2.⁽¹⁰⁾

We now consider the effect of a single weak impurity at the origin ($x=0$). In this limit, a small portion of quasiparticles backscatter, and the role of fractional charge is most transparent. In the generic case involving no spin polarization or spin flip, local weak backscattering processes may be described by:

$$H_{imp} = \sum_{\alpha} \left\{ \sum_{i=1,2} u_i [\psi_{Ri\alpha}^{\dagger}(0) \psi_{Li\alpha}(0) + \text{h.c.}] + u_3 [\psi_{R1\alpha}^{\dagger}(0) \psi_{L2\alpha}(0) + \text{h.c.}] \right. \\ \left. + u_4 [\psi_{R2\alpha}^{\dagger}(0) \psi_{L1\alpha}(0) + \text{h.c.}] \right\} \quad (5)$$

where $\alpha = \uparrow, \downarrow$, ‘‘h.c.’’ denotes Hermitian conjugation, u_1 and u_2 are weak intra-subband scattering potentials, and u_3 and u_4 describe the inter-subband scattering. Processes associated with u_1 and u_2 conserve all particle numbers while the u_3 and u_4 scattering terms do not conserve ρ - and σ -particle numbers (these arise physically for impurities which break the sublattice-reflection symmetry of the graphene lattice).

We note that the bosonized version of Eq. (5) may be expressed in terms of right and left moving creation and annihilation operators $e^{\pm i\Phi_a^{R/L}}$ that describe the freely propagating chiral excitations of the system; the impurity site can create, destroy, or backscatter these excitations. Most importantly, every scattering process possesses a term of the form $e^{\pm i\Phi_{\rho+}^R} e^{\mp i\Phi_{\rho+}^L}$, reflecting the fact that a quasiparticle characterized by the creation operator $e^{-i\Phi_{\rho+}^{R/L}}$ is always backscattered. As detailed in ref. 12, the operator $e^{i\Phi_{\rho+}^{R/L}}$ creates a kink of magnitude πg in $\Phi_{\rho+}^R$ at $x=0$, or

equivalently, a peak in $n_{\rho+}^T$ of magnitude g . Therefore, the magnitude of the fractional charge associated with the impurity backscattering is “ ge .”

Finally we consider the real time, finite temperature action applicable at the impurity site. The manner in which we employ it parallels the treatment in ref. 13. We integrate out the ϕ_a variables from the bulk Hamiltonian (though, where appropriate, we integrate out θ_a variables instead), and then integrate out fluctuations away from the impurity as in ref. 14. Using the Keldysh approach,⁽¹⁵⁾ we write the partition function in terms of time dependent backward and forward paths $\theta^\pm \equiv \theta \pm \frac{1}{2}\tilde{\theta}$:

$$\mathcal{Z} = \int \prod_a \mathcal{D}\theta_a^+ \mathcal{D}\theta_a^- e^S \quad (6)$$

with $a = (\rho+, \rho-, \sigma+, \sigma-)$. The action $S = S_0 + S_1 + S_2$ is given by

$$\begin{aligned} S_0 &= -\sum_a \left[\frac{1}{\pi g_a} \int d\omega \omega \coth\left(\frac{\omega}{2kT}\right) |\tilde{\theta}_a(\omega)|^2 + \frac{2i}{\pi g_a} \int dt \tilde{\theta}_a(t) \dot{\theta}_a(t) \right] \\ S_1 &= -i \sum_{js} \int dt [f(\Gamma_{js}^+(t)) - f(\Gamma_{js}^-(t))] \\ S_2 &= i \frac{2}{\pi} \int dt [A(t) \dot{\tilde{\theta}}_{\rho+}(t) + \eta(t) \dot{\theta}_{\rho+}(t)] \end{aligned} \quad (7)$$

Here, S_0 describes the unperturbed system. S_1 is derived from the impurity Hamiltonian of Eq. (5). The Γ_{js}^\pm operators are defined for $j=1 \dots 4$ and $s = \pm 1$:

$$\begin{aligned} \Gamma_{1s} &= \theta_{\rho+} + s\theta_{\sigma+} + \theta_{\rho-} + s\theta_{\sigma-} \\ \Gamma_{2s} &= \theta_{\rho+} + s\theta_{\sigma+} - \theta_{\rho-} - s\theta_{\sigma-} \\ \Gamma_{3s} &= \theta_{\rho+} + s\theta_{\sigma+} + \phi_{\rho-} + s\phi_{\sigma-} \\ \Gamma_{4s} &= \theta_{\rho+} + s\theta_{\sigma+} - \phi_{\rho-} - s\phi_{\sigma-} \end{aligned} \quad (8)$$

where the \pm superscripts which denote backward and forward paths are suppressed for all variables. S_2 originates from coupling the physical current to an external source of voltage \dot{A} .

3. PHYSICAL PROPERTIES

An analysis of the nanotube with a single impurity, schematically shown in Figs.1 and 2, serves to bring out striking Luttinger liquid

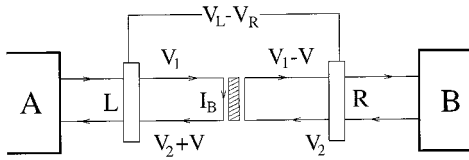


Fig. 1. Quasiparticle transport in a nanotube with a single impurity. The current enters the nanotubes through the external contacts A and B while the two voltage probes L and R serve to measure the voltage drop across the impurity. Chiral modes are shown for clarity of expression, but they cannot be probed separately as the voltage probes couple to both right- and left-movers.

features. However, in the absence of the impurity, the conductance *measured across the external contacts* A and B , which we assume to be adiabatic, is $G = 4(e^2/h)$,⁽¹⁶⁾ appropriate for a non-interacting one-dimensional system with four channels for conductance. Effectively, this is due to the fact that though an isolated nanotube would have an associated conductance $4g(e^2/h)$, the external metallic contacts are three-dimensional Fermi liquids, and the observed conductance involves electrons backscattering at the interface.⁽¹⁶⁾

Weak backscattering in the presence of the impurity causes a reduction in the conductance. For a temperature $kT \gg (\hbar v_F/\ell)$ (k is Boltzmann's constant), where ℓ is the distance from the impurity to the nearest contact (A or B), the reduction has the form $\delta G(T) \propto -u^2 T^{2A-2}$, where $A = \frac{1}{4}(g+3)$, and " u " is the impurity strength.⁽¹²⁾ Given the estimate $g = 0.2$ for the nanotube,⁽¹⁰⁾ $\delta G(T) \propto T^{-0.4}$ ought to be observable across a wide temperature range. Similar considerations for the limit of large tunneling barrier, where only few electrons tunnel through, show that an infinite wire reflects electrons completely at $T=0$. However, at finite temperature it exhibits the temperature dependence $G \propto T^{2\lambda-2}$, where $\lambda = \frac{1}{4}(1/g+3)$.

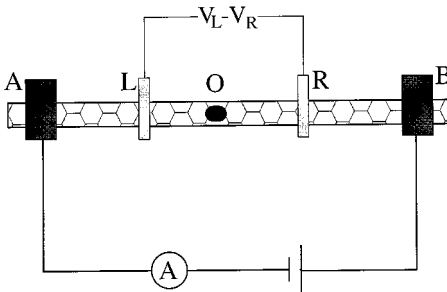


Fig. 2. Experimental set-up: a nanotube with an impurity at point "O" is connected in series with an ammeter and a d.c. source supply. The current enters into the nanotube through the external contacts A and B . A voltmeter is connected across probes L and R .

As seen in Figs. 1 and 2, the current contributing to the conductance involves right moving quasiparticles emerging from the left lead, and left movers from the right lead. As emphasized by the chiral decomposition of the previous section, the quasiparticles carry fractional charge ge , and a portion of them is backscattered into the lead from which they emerge. In the presence of an externally applied potential, the right and left moving chiral modes maintain a difference in chemical potential, $V_1 - V_2 - V$. The potential difference $V_{12} = V_1 - V_2$ between the chiral modes arises in the presence of an external bias voltage. In the absence of the impurity, the current I_0 flowing across the wire is given by $I_0 = 4g(e^2/h) V_{12}$. Unfortunately, unlike in the quantum Hall case, where the right- and left-movers are spatially separated, and V_{12} is measurable,⁽⁴⁾ here the leads couple to both modes. Thus, V_{12} cannot be measured, and the ideal conductance $4g(e^2/h)$ cannot be extracted.

The voltage drop V is caused by the backscattering of quasiparticles. The net current traversing the wire in the presence of the impurity is given by

$$\begin{aligned} I &= I_0 - I_B \\ &= 4g \frac{e^2}{h} (V_{12} - V) \end{aligned} \quad (9)$$

where V is the voltage drop across the impurity, and $I_B = 4g(e^2/h) V$ is the backscattered current. Also, as we work in the weak backscattering limit, we have $I_B \ll I_0$. Equation (9) can be either derived from the action of Eq. (7) by calculating the average current $I = \langle 2e\dot{\theta}/\pi \rangle$ as the functional derivative $-i(\delta Z/\delta\eta)$, or by simple consideration of chiral mode properties, as in the case of spinless fermions.⁽¹²⁾ In our set-up, we find that $V_{12} = (h/e) \dot{A}$, and V is the expectation value of the voltage operator given by

$$\hat{V} = \frac{1}{4} \frac{h}{e} \sum_{js} u_j \sin(\Gamma_{js} + gA) \quad (10)$$

with Γ 's defined in Eq. (8).

The role of fractional charge is made manifest in the shot noise generated by the quasiparticles striking the impurity. To derive the general behavior of C_I at finite temperature, we define the correlation function $C_{\mathcal{O}}$ in the quantity " \mathcal{O} ,"

$$C_{\mathcal{O}}(\omega) = \frac{1}{2} \int dt e^{i\omega t} \langle \{ \mathcal{O}(t), \mathcal{O}(0) \} \rangle \quad (11)$$

and use Eq. (7) as in ref. 13 to obtain a relation between current and voltage fluctuations, C_I and C_V respectively. At low temperature, and in the limit of zero frequency, this becomes

$$C_I = \left(\frac{4ge^2}{h}\right)^2 C_V(\omega) + 2kT \frac{dI}{dV_{12}} - \left(\frac{4ge^2}{h}\right) 2kT \frac{dV}{dV_{12}} \quad (12)$$

We then perturbatively calculate the voltage correlations to lowest non-vanishing order in the impurity scattering potential to obtain

$$C_V(\omega \rightarrow 0) = \frac{h}{4e} \coth\left(\frac{geV_{12}}{2kT}\right) \langle \hat{V} \rangle \quad (13)$$

We observe that the noise due to voltage fluctuations is partitioned between four channels. Putting together Eqs. (9), (12) and (13), we obtain the desired form of C_I :

$$C_I(\omega \rightarrow 0) = ge \coth\left(\frac{geV_{12}}{2kT}\right) I_B + 2kT \frac{dI}{dV_{12}} - 2kT \frac{dI_B}{dV_{12}} \quad (14)$$

Setting $T=0$, we see that C_I has the celebrated shot noise form geI_B . It exhibits crossover from shot noise to thermal noise when the condition $geV_{12} \approx 2kT$ is satisfied. Eq. (14) offers a tractable starting point for experimental data analysis.

4. EXPERIMENT

A possible experimental configuration which realizes Fig. 1 is shown in the four-probe geometry of Fig. 2. As elucidated in what follows, two sets of measurements, one in the absence of the impurity and one in its presence, enable one to extract the shot noise C_I of Eq. (12), and the voltage V of Eq. (9) generated across the impurity. These two quantities in turn suffice to extract the charge fraction “ g .” In the proposed set-up, an external supply maintains a voltage bias between the ends of the nanotube and drives the current through it, while an ammeter measures this net current I . A voltmeter across LR measures the difference in potential $V_{LR} = V_L - V_R$ (see Fig. 2). As measurements involve both the absence and the presence of the impurity, this impurity would have to be created in a controlled way such as by means of an AFM tip.⁽⁹⁾

The conditions in which the experiment ought to be performed are rather specific, but feasible. We assume that the probes L and R are non-invasive in their contribution to voltage drops, and that backscattering at

all leads is small. The small backscattering condition is equivalent to the requirement that the two-terminal resistance of the entire wire is close to the ideal value of $h/4e^2 \approx 6.25k\Omega$. We also require the further condition $eV_{12}, kT \gg \hbar v_{p+}/\ell$. This ensures that the one-dimensional physics of the tube is probed as opposed to that of the three-dimensional external contacts, in essence that quasiparticle propagation is not coherent across the entire system. Finally, we make the reasonable assumption that heat generated in the external circuit is removed by phonons, hence maintaining steady temperature T , and that the noise in it has the current-independent Johnson–Nyquist form $C_{\text{ext}} \sim kT/R_{\text{ext}}$, where R_{ext} is the resistance of the external circuit.⁽¹⁷⁾

Determining C_I , the noise across the impurity, proves a tricky task due to multiple noise sources, and particularly due to possible correlations with scattering at the leads. But taking into account the conditions assumed above for ℓ and for the transmission at the leads, as well as the fact that the weak impurity also has large transmission, we find the noise to be additive. In other words, one can measure the current noise in the circuit in the presence and absence of the impurity, C_I^{imp} and C_I^0 respectively, keeping the mean current in the circuit fixed. Then, the shot noise across the impurity would just be their difference; $C_I = C_I^{\text{imp}} - C_I^0$.

One could determine the voltage V generated across the impurity by merely measuring the voltage V_{LR} of Figs. 1 and 2 across it if the leads L and R coupled to right- and left-movers (see Figs. 1 and 2) symmetrically. However, as shown below, even if this coupling is asymmetric, for fixed current I , the voltage V is simply the difference between the voltages V_{LR} and V_{LR}^0 measured across LR in the presence and in the absence of the impurity, respectively. To see this, let a_R and $1 - a_R$ be the fractions with which the right lead couples to the right- and left-movers respectively, and similarly for the left lead. We assume a_R and a_L are voltage-independent, a reasonable assumption given the extremely large ($\mathcal{O}(eV)$) electronic energy scales involved in the microscopic matrix elements which determine this coupling. With reference to the voltages shown in Fig. 1, we then have

$$\begin{aligned} V_R &= a_R(V_1 - V) + (1 - a_R)V_2 \\ V_L &= a_L V_1 + (1 - a_L)(V_2 + V) \\ V_{LR} &= V + (a_L - a_R)(V_1 - V_2 - V) \end{aligned} \quad (15)$$

with the total current in the circuit given by

$$I = 4g \frac{e^2}{h} (V_1 - V_2 - V) \quad (16)$$

In the absence of the impurity, setting $V=0$, we have

$$V_{LR}^0 = (a_L - a_R)(V_1^0 - V_2^0) \quad (17)$$

and the corresponding current

$$I_0 = 4g \frac{e^2}{h} (V_1^0 - V_2^0) \quad (18)$$

Finally, for fixed current $I = I_0$, Eqs. (15)–(18) give the required form for V ,

$$V = V_{LR} - V_{LR}^0 \quad (19)$$

Now, in the limit $kT \ll V_{12}$ (which is of comparable magnitude to the actual applied voltage), Eq. (14) takes the form $C_I = geI_B$. Since $I_B = (4ge^2/h) V$, we have

$$C_I = 4g^2 \frac{e^3}{h} V \quad (20)$$

Equation (20) enables an experimental determination of “ g ,” given the measured quantities C_I and V . We emphasize that the physical appearance of “ g^2 ” in Eq. (20) has two distinct physical origins. As seen from the relation $I_B = (4ge^2/h) V$, one factor of g simply reflects the reduced intrinsic conductance of the Luttinger liquid. The second factor of g (in $C_I = geI_B$) directly follows from the fractional charge ge of the current-carrying solitons. It is in this sense that Eq. (20) is a direct measure of fractional quasiparticle charge.

In the quantum Hall system, determining fractional charge and observing crossover from shot noise to thermal noise were performed in a clear-cut fashion through finite temperature measurements⁽⁴⁾ that conformed to the noise described by the analog of Eq. (14). Here, precise quantities cannot be extracted due to the facts that a_R and a_L of Eqs. (15) and (17) are unknown, and that V_{12} cannot be measured. However, measurements at different values of the average current I , and less easily at different temperatures T , would not only probe quasiparticle charge, they would also display the clear dependence of noise on thermal effects. Also, while a gate voltage across the Hall bar allowed one to tune the backscattering strength elegantly, here one could change the barrier strength described in Eq. (5) in a less straightforward way by studying different impurities.

6. CONCLUSION

The single-walled armchair nanotube hosts a fine arena for observing many of the intriguing features of a four channel Luttinger liquid. Its contrast with Fermi liquids becomes strikingly apparent when its transport properties in the presence of an impurity are compared with Landauer transport theory.⁽¹⁸⁾ Non-equilibrium measurements serve to bring out the fractional nature of the charge carried by the quasiparticle excitations in the nanotube.

Rapid progress in experimental techniques offers scope for studying interacting one-dimensional systems in interesting geometries. For instance, a finite length tube would exhibit resonances in spectral features.⁽¹⁰⁾ A nanotube bearing two (or more) impurities could display resonant tunneling and plateaus in conductance, as observed in thin wires.⁽¹⁹⁾ Fabrication of nanotubes with crossed geometries⁽²⁰⁾ allows for observing quantum statistics of the constituent particles via the Hanbury Brown–Twiss effect as was studied in the quantum Hall system by Henny *et al.*, who used a four terminal geometry to measure shot noise and demonstrate the fluctuation-dissipation relation.⁽²¹⁾

ACKNOWLEDGMENTS

Thanks to C. Dekker for inspiring this study. This research was supported by NSF Grants DMR-9985255, DMR-97-04005, DMR95-28578, PHY94-07194 and by Broida Excellence Fellowship, Fernando–Fithian Fellowship and Parsons Foundation Fellowship.

REFERENCES

1. S. Tomonaga, *Prog. Theor. Phys. (Kyoto)* **5**:544 (1950); J. M. Luttinger, *J. Math. Phys. (N.Y.)* **4**:1154 (1963).
2. F. D. M. Haldane, *J. Phys. C* **14**:2585 (1981); *Phys. Rev. Lett.* **47**:1840 (1981).
3. X. G. Wen, *Phys. Rev. B* **43**:11025 (1991); *Phys. Rev. Lett.* **64**, 2206 (1990); *Phys. Rev. B* **44**:5708 (1991).
4. L. Saminadayar, D. C. Glattli, Y. Jin, and B. Etienne, cond-mat/9706307; R. de Picciotto, M. Reznikov, M. Heiblum, V. Umansky, G. Bunin, and D. Mahalu, *Nature* **389**:162 (1997).
5. Z. Yao, C. L. Kane, and C. Dekker, cond-mat/9911186.
6. C. Dekker, *Physics Today* **52**:22 (1999).
7. M. Bockrath, D. H. Cobden, J. Lu, A. G. Rinzler, R. E. Smalley, L. Balents, and P. L. McEuen, *Nature* **397**:598 (1999).
8. Z. Yao, H. Postma, L. Balents, and C. Dekker, *Nature* **402**:273 (1999).
9. H. Postma, M. de Jonge, Z. Yao, and C. Dekker, Cond-mat/0009055.
10. C. L. Kane, L. Balents, and M. P. A. Fisher, *Phys. Rev. Lett.* **79**:5086 (1997).
11. R. Egger and A. Gogolin, *Phys. Rev. Lett.* **79**:5082 (1997).

12. M. P. A. Fisher and L. I. Glazman, *Mes. Elec. Transp.*, L. L. Sohn, L. P. Kouwenhoven, and G. Schon, eds. (Kluwer Academic Publishing, Dordrecht, 1997), NATO Series E, Vol. 345, p. 331.
13. C. L. Kane and M. P. A. Fisher, *Phys. Rev. Lett.* **72**:724 (1994).
14. C. L. Kane and M. P. A. Fisher, *Phys. Rev. B* **46**:15233 (1992).
15. L. V. Keldysh, *ZhETF* **47**:1515 (1964) [*Sov. Phys. JETP* **20**:1018 (1965)]; M. P. A. Fisher and W. Zwerger, *Phys. Rev. B* **32**:6190 (1985).
16. D. L. Maslov and M. Stone, *Phys. Rev. B* **52**:5539 (1995); I. Safi and H. J. Schulz, *Phys. Rev. B* **52**:17040 (1995); V. V. Ponomarenko, *Phys. Rev. Lett.* **52**:8666 (1995).
17. A. H. Steinbach, J. M. Martinis, and M. H. Devoret, *Phys. Rev. Lett.* **76**:3806 (1996).
18. R. Landauer, *Philos. Mag.* **21**:863 (1970); *Physica (Amsterdam)* **38D**:226 (1989); M. Buettiker, *Phys. Rev. Lett.* **57**:1761 (1986); *Phys. Rev. Lett.* **65**:2901 (1990); *Phys. Rev. B* **46**:12485 (1992).
19. See for, e.g., O. M. Auslaender, A. Yacoby, R. de Picciotto, K. W. Baldwin, L. N. Pfeiffer and K. W. West, cond-mat/9909138.
20. J. Kim, K. Kang, J. O. Lee, K. H. Yoo, J. R. Kim, J. W. Park, H. M. So, and J. J. Kim, cond-mat/0005083.
21. M. Henny, S. Oberholzer, C. Strunk, T. Heinzl, K. Ensslin, M. Holland, and C. Schonberger, *Science* **284**:296 (1999).